Molecules and Cells

C9orf72-Associated Arginine-Rich Dipeptide Repeat Proteins Reduce the Number of Golgi Outposts and Dendritic Branches in *Drosophila* Neurons

Jeong Hyang Park[1,2,5], Chang Geon Chung[1,2,5], Jinsoo Seo[1,2], Byung-Hoon Lee[2,3], Young-Sam Lee[2,3,4], Jung Hyun Kweon[1,*], and Sung Bae Lee[1,2,4,*]

[1]Department of Brain & Cognitive Sciences, Daegu Gyeongbuk Institute of Science & Technology (DGIST), Daegu 42988, Korea, [2]Protein Dynamics-Based Proteotoxicity Control Laboratory, Basic Research Lab, DGIST, Daegu 42988, Korea, [3]Department of New Biology, DGIST, Daegu 42988, Korea, [4]Well Aging Research Center, Division of Biotechnology, DGIST, Daegu 42988, Korea, [5]These authors contributed equally to this work.
*Correspondence: kweonie1126@gmail.com (JHK); sblee@dgist.ac.kr (SBL)
https://doi.org/10.14348/molcells.2020.0130
www.molcells.org

Altered dendritic morphology is frequently observed in various neurological disorders including amyotrophic lateral sclerosis (ALS) and frontotemporal dementia (FTD), but the cellular and molecular basis underlying these pathogenic dendritic abnormalities remains largely unclear. In this study, we investigated dendritic morphological defects caused by dipeptide repeat protein (DPR) toxicity associated with G4C2 expansion mutation of *C9orf72* (the leading genetic cause of ALS and FTD) in *Drosophila* neurons and characterized the underlying pathogenic mechanisms. Among the five DPRs produced by repeat-associated non-ATG translation of G4C2 repeats, we found that arginine-rich DPRs (PR and GR) led to the most significant reduction in dendritic branches and plasma membrane (PM) supply in Class IV dendritic arborization (C4 da) neurons. Furthermore, expression of PR and GR reduced the number of Golgi outposts (GOPs) in dendrites. In *Drosophila* brains, expression of PR, but not GR, led to a significant reduction in the mRNA level of *CrebA*, a transcription factor regulating the formation of GOPs. Overexpressing *CrebA* in PR-expressing C4 da neurons mitigated PM supply defects and restored the number of GOPs, but the number of dendritic branches remained unchanged, suggesting that other molecules besides CrebA may be involved in dendritic branching. Taken together, our results provide valuable insight into the understanding of dendritic pathology associated with C9-ALS/FTD.

Keywords: amyotrophic lateral sclerosis, *C9orf72*, CrebA, dendrites, Golgi outposts

INTRODUCTION

Many neurological disorders have a number of common pathological features, suggesting that they may share a mechanistic origin. Abnormal dendritic morphology, which is thought to precede neuronal cell death, is one such feature (Kulkarni and Firestein, 2012; Kweon et al., 2017). Even amyotrophic lateral sclerosis (ALS), the pathological hallmark of which is motor neuron axonal degeneration (Fischer and Glass, 2007; Saberi et al., 2015; Taylor et al., 2016), has this characteristic. More than two decades ago, abnormal den-

Received 11 June, 2020; revised 13 August, 2020; accepted 30 August, 2020; published online 17 September, 2020

eISSN: 0219-1032

dritic abnormality was first identified in ALS (Karpati et al., 1988; Nakano and Hirano, 1987; Takeda et al., 2014). Since then, some of the ALS-associated mutations in *TARDBP* and *FUS* have been linked to dendritic defects (Herzog et al., 2017; Tibshirani et al., 2017), but our understanding of the mechanism underlying these defects remains poor. Similarly, frontotemporal dementia (FTD), which is considered to be on the same disease spectrum as ALS because they have a shared set of genes and symptoms (Ling et al., 2013), also manifests dendritic abnormality. A study in 1999 showed that the complexity and number of dendritic branches were reduced in both pyramidal and non-pyramidal neurons from FTD postmortem brain samples (Ferrer, 1999). Surprisingly, very few studies since have examined the mechanism underlying dendritic pathology in FTD.

The most common genetic cause of both ALS and FTD is the intronic hexanucleotide (G4C2) repeat expansion mutation in *C9orf72* (DeJesus-Hernandez et al., 2011; Renton et al., 2011). Repeat expansions greater than 30 are understood to be pathogenic, whereas fewer than 30 repeats are found in most healthy controls (Renton et al., 2011). These repeated sequences can be transcribed in both sense and antisense directions, and repeat RNA products of both often form nuclear foci where several RNA-binding proteins are sequestered (Lee et al., 2013; Xu et al., 2013). Some of these repeat RNAs exit the nucleus and undergo repeat-associated non-ATG (RAN) translation into five dipeptide repeat proteins (DPRs). Among the five DPRs, glycine-arginine (GR) and proline-arginine (PR) are most toxic; glycine-alanine (GA) is moderately toxic; and glycine-proline (GP) and proline-alanine (PA) are relatively benign (Freibaum and Taylor, 2017). Whether the arginine-rich DPRs can induce dendritic defects is not known.

Recently, Golgi outposts (GOPs) have been associated with dendritic defects in *Drosophila* models for Machado-Joseph Disease, spinocerebellar ataxia 1 and Huntington's disease (Chung et al., 2017). In that study, nuclear polyQ proteins interfered with the CREB-binding protein (CBP)-CrebA pathway, thereby reducing the number of GOPs and decreasing plasma membrane (PM) supply in dendrites. Interestingly, a chimeric protein comprising green fluorescent protein (GFP) fused to a fragment of Golgi Complex Protein in COS-7 cells has been shown to form nuclear aggregates and recruit proteins such as CBP into the inclusion (Fu et al., 2005). This study suggests that when accumulated in the nucleus, aberrant non-polyQ proteins may also induce dysregulation of the CBP-CrebA pathway, leading to dendritic defects. Arginine-rich DPRs GR and PR are known to accumulate in the nuclei of many cell types (Kwon et al., 2014; Lee et al., 2016; Rudich et al., 2017; Wen et al., 2014), suggesting that they may induce dendritic defects via dysregulation of the CBP-CrebA pathway. Several previous studies have used *Drosophila* larval Class IV dendritic arborization (C4 da) neurons to study dendritic pathology (Chung et al., 2017; Kwon et al., 2018; Lee et al., 2011; Lin et al., 2015). The usefulness of the C4 da neuronal system stems from its sharing similar mechanisms for dendritic arborization with mammalian neurons and its amenability to *in vivo* single cell imaging (Jan and Jan, 2010; Kweon et al., 2017). In this study, we used C4 da neurons as a model in which to investigate abnormal dendritic morphology induced by DPR toxicity.

MATERIALS AND METHODS

Drosophila stocks and gene switch-mediated expression

All flies were maintained at 25°C and 60% humidity. The following lines were obtained from Bloomington *Drosophila* Stock Center (USA): w^{1118} (3605), *UAS-PR36* (58694), *UAS-GR36* (58692), *UAS-GA36* (58693), *UAS-PA36* (58695), *UAS-RO288* (58681), *UAS-CrebA* (32572), *UAS-GalT-RFP* (65251), *GMR-gal4* (1104), and *elav-gal4* (8760). *UAS-ManII-eGFP*; *UAS-CD4-tdTOM*, *UAS-CD4-tdGFP*, ppk^{1a}*-gal4*, *GS-*ppk^{1a}*-gal4*, and *ppk-UAS-CD4-tdTOM* were provided by Yuh Nung Jan (University of California, San Francisco [UCSF], USA). To activate gene switch-mediated transcription of gal4, adult flies were fed food with RU486 (100 μM RU486 dissolved in 80% ethanol) for 15 days.

Generation of *Drosophila* transgenic construct

To control for gal4 dilution, transgenic flies carrying empty pACU2 vector (provided by Yuh Nung Jan; UCSF) were generated by BestGene (USA). The empty vector is inserted in the second chromosome at VK02 site. This transgene (*UAS-empty*) was used as a control in *Drosophila* retinal imaging study.

Drosophila retinal imaging

Leica SP5 was used to take *Drosophila* retinal images. Upon dissection, the retinas (left only) were imaged at 160× magnification.

Immunohistochemistry

Third instar larvae or adult flies were dissected and fixed with 3.7% formaldehyde for 20 min at room temperature. After washing with phosphate-buffered saline (PBS), the larval fillets were incubated in a blocking buffer for 45 min. Next, the fillets were incubated in the primary antibody overnight at 4°C. The following primary antibodies were used: α-polyPR (23979-1-AP, 1:20; Proteintech, USA) and α-RFP (#ab62341, 1:400; Abcam, UK). Fillets were then washed with washing buffer three times for 5 min each. Then, they were further incubated in the secondary antibody for 3 h at room temperature. The following secondary antibodies were used: goat α-mouse Alexa 555 (A28180, 1:400; Thermo Fisher Scientific, USA), goat α-rabbit Alexa 647 (A21244, 1:200; Thermo Fisher Scientific) and goat α-Horseradish Peroxidase (123-545-021, 1:200; Jackson ImmunoResearch, USA). Fillets were washed five times with washing buffer prior to mounting on a slide glass for imaging.

Confocal microscopy

Images of C4 da neurons in larvae or adult flies after immunohistochemistry and in larvae *in vivo* were obtained using Zeiss LSM700 or LSM780 confocal microscopy (Zeiss, Germany). All images of the C4 da neurons were acquired from abdominal A2-A6 segments.

Reverse transcriptase polymerase chain reaction (RT-PCR)

Total RNA was extracted from the heads of *Drosophila* with

the following genotypes: *w*^{1118}*/elav-gal4*, *UAS-PR36/elav-gal4*, and *UAS-GR36/elav-gal4*. Concentration of total RNA of each sample was measured by NanoDrop spectrophotometer (Thermo Fisher Scientific). 18S rRNA was used as a reference for normalizing *CrebA* mRNA level.

Primer sequences for *CrebA*:

5'- CAACTACCTCAGCACCTATACGAC
3'- GTTACCTTCGGAATCATCGCTGG

Dendrite analysis

All images of dendrites were first converted into skeletal images using ImageJ. Then, those images were used to measure dendritic length and branch points.

Quantification of CD4-tdGFP intensity

Images obtained from confocal microscopy were processed using Zen black program, Adobe Photoshop CC and Im-

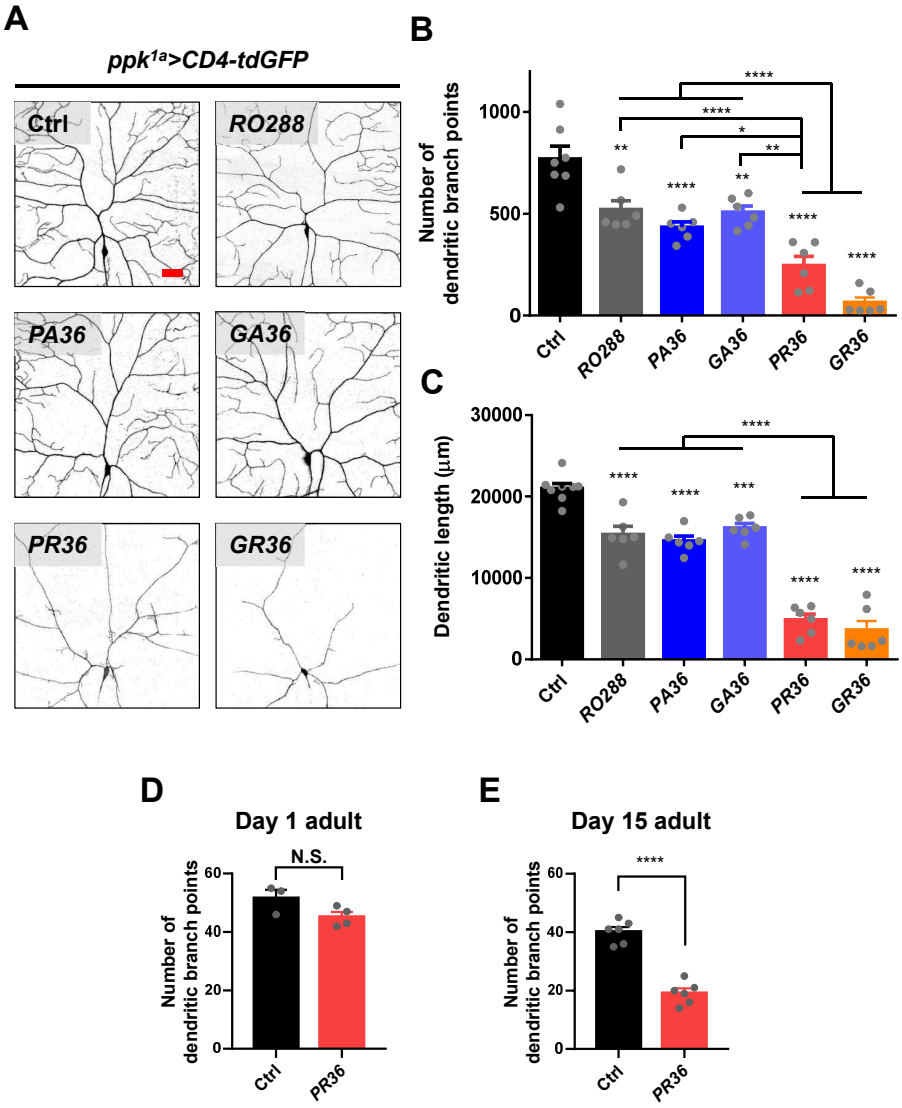

Fig. 1. Arginine-rich DPRs induce dendritic defects in *Drosophila* C4 da neurons. (A) Representative images of dendrites of C4 da neurons of control (Ctrl) or expressing the denoted transgenes (Genotype: **Ctrl**, +/+;*ppk*^{1a}*>UAS-CD4-tdGFP/+*; ***RO288***, *UAS-RO288/+;ppk*^{1a}*>UAS-CD4-tdGFP/+*; ***PA36***, *UAS-PA36/+;ppk*^{1a}*>UAS-CD4-tdGFP/+*; ***GA36***, *UAS-GA36/+;ppk*^{1a}*>UAS-CD4-tdGFP/+*; ***PR36***, *UAS-PR36/+;ppk*^{1a}*>UAS-CD4-tdGFP/+*; ***GR36***, *UAS-GR36/+;ppk*^{1a}*>UAS-CD4-tdGFP/+*). Scale bar = 20 μm. (B) Quantification of the dendritic branch points of neurons expressing the denoted transgenes described in Fig. 1A. $*P < 0.05$, $**P < 0.01$, $****P < 0.0001$ by two-tailed *t*-test; error bars ± SEM; n ≥ 6 neurons. (C) Quantification of the dendritic length of neurons expressing the denoted transgenes described in Fig. 1A. $***P < 0.001$, $****P < 0.0001$ by two-tailed *t*-test; error bars ± SEM; n ≥ 6 neurons. (D) Quantification of the number of dendritic branch points in C4 da neurons of Ctrl or expressing *PR36* at 1 day after eclosion (Genotype: **Ctrl**, +/+;*GS-ppk*^{1a}*,ppk-UAS-CD4-tdTOM/+*; ***PR36***, *UAS-PR36/+;GS-ppk*^{1a}*,ppk-UAS-CD4-tdTOM/+*). N.S., not significant, $P = 0.0918$ by two-tailed *t*-test; error bars ± SEM; n ≥ 3 neurons. (E) Quantification of the number of dendritic branch points in C4 da neurons of Ctrl or expressing *PR36* at 15 day after RU486-mediated transcriptional activation of gal4. $****P < 0.0001$ by two-tailed *t*-test; error bars ± SEM; n = 6 neurons.

ageJ. ImageJ→Plugin→NucMed→Lookup table→Blue Green Red was used for GFP intensity quantification. Then, the whole dendritic area of C4 da neurons was selected and its CD4-tdGFP intensity was analyzed using histogram plug-in in the ImageJ software. All images presented in the same panel were processed in the same manner.

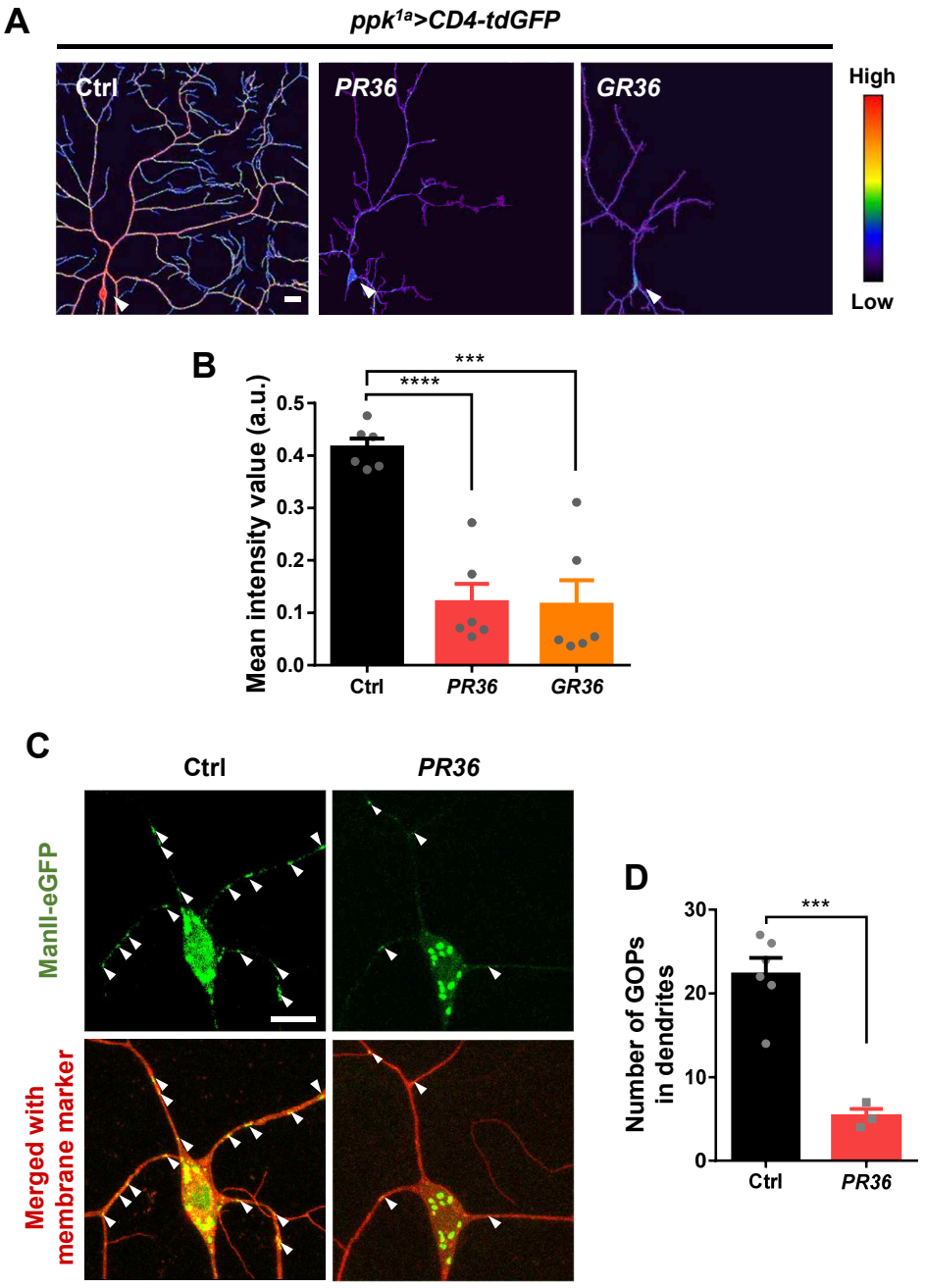

Fig. 2. Arginine-rich DPRs impair PM supply and reduce the number of GOPs in C4 da neurons. (A) Representative CD4-tdGFP-labeled dendrite images (pseudo-colored) in C4 da neurons expressing denoted DPR transgenes (Genotype: **Ctrl**, +/+;*ppk*^{1a}*>UAS-CD4-tdGFP/+*; ***PR36***, *UAS-PR36/+;ppk*^{1a}*>UAS-CD4-tdGFP/+*; ***GR36***, *UAS-GR36/+;ppk*^{1a}*>UAS-CD4-tdGFP/+*). White arrowheads indicate soma of neurons. Scale bar = 20 μm. (B) Quantification of the intensity value of membrane-targeted fluorescence proteins (CD4-tdGFP) in C4 da neurons expressing denoted DPR transgenes described in Fig. 2A. ***P = 0.0001, ****P < 0.0001 by two-tailed t-test; error bars ± SEM; n = 6 neurons. (C) Representative images of GOPs (marked by *medial*-Golgi marker ManII-eGFP) in C4 da neurons of Ctrl or expressing *PR36* (Genotype: **Ctrl**, *UAS-ManII-eGFP/+;ppk*^{1a}*>UAS-CD4-tdTOM/+*; ***PR36***, *UAS-PR36/UAS-ManII-eGFP;ppk*^{1a}*>UAS-CD4-tdTOM/+*). White arrowheads indicate GOPs. Scale bar = 10 μm. (D) Quantification of the number of GOPs in C4 da neurons of Ctrl or expressing *PR36* described in Fig. 2C. ***P = 0.0006 by two-tailed t-test; error bars ± SEM; n ≥ 3 neurons.

Statistical analysis

Statistical analysis was done using GraphPad Prism 7 (GraphPad Software, USA). Depending on the data, we applied Student's *t*-test followed by Tukey's post-hoc analysis. In all figures, not significant (N.S.), *, **, ***, and **** represent $P > 0.05$, $P < 0.05$, $P < 0.01$, $P < 0.001$, and $P < 0.0001$, respectively. Error bars are SEM.

RESULTS

Arginine-rich DPRs induce loss of dendritic branch points in *Drosophila* C4 da neurons

Among the five types of DPRs produced by RAN translation from G4C2 repeat RNA, we tested four of them (PA, GA, PR, and GR) for their effect on dendritic morphology in *Drosophila* C4 da neurons. GP was not tested due to lack of an available fly line and because it is known to be benign in various model systems (Freibaum and Taylor, 2017). Additionally, we also tested G4C2 RNA only (RO288) transgene to examine the effect of RNA toxicity on dendritic morphology. Expression of arginine-rich DPRs *PR36* and *GR36* in C4 da neurons via a *ppk*^{1a}*-gal4* driver led to a noticeable decrease in the number of dendritic branch points compared to the controls, whereas expression of *PA36*, *GA36,* and *RO288* did not (Fig. 1A). However, when we quantified the number of dendritic branch points in DPR-expressing neurons, we found that even expression of *PA36*, *GA36*, and *RO288* led to a significant decrease compared to *wildtype* controls (Ctrl) (Fig. 1B). Notably, C4 da neurons expressing *PR36* and *GR36* showed considerably fewer dendritic branch points compared to the Ctrl or those expressing *PA36*, *GA36*, and *RO288* (Fig. 1B). Likewise, expression of *PA36*, *GA36*, and *RO288* significantly decreased the total dendritic length compared to Ctrl, whereas *PR36* and *GR36* expression led to an even shorter total dendritic length (Fig. 1C). However, expression of DPRs induced no morphological abnormality in the pattern of axon scaffold in the larval ventral nerve cord (Supplementary Fig. S1).

Because ALS/FTD is an adult onset neurodegenerative disease, we decided to test whether arginine-rich DPR expression can induce dendritic defects in fully developed adult flies. To this end, we conditionally expressed *PR36* in adult C4 da neurons using *GS-ppk*^{1a}*-gal4*—a RU486-inducible gene switch *gal4*. At day 1, we observed no dendritic changes in flies with the *PR36* transgene compared to the controls (Fig. 1D) because the transcriptional activity of gal4 was not yet induced. After 15 days of induction, the adult C4 da neurons expressing *PR36* showed a significant reduction in the number of dendritic branch points (Fig. 1E). These results suggest that *PR36* expression can induce non-developmental dendritic phenotypes in the adult *Drosophila* C4 da neurons.

Arginine-rich DPRs disrupt PM supply and induce a loss of GOPs in *Drosophila* C4 da neurons

We also noticed a significant decrease in the fluorescence intensity of CD4-tdGFP in C4 da neurons expressing arginine-rich DPRs compared to the controls (Figs. 2A and 2B, Supplementary Fig. S1). Expression of *PA36* and *GA36* did not alter the fluorescence intensity of CD4-tdGFP (Supplementary Fig. S2). Interestingly, decrease in fluorescence intensity of transgenic PM marker proteins has been closely associated with reduced PM supply (Chung et al., 2017; Murthy et al., 2005), suggesting that arginine-rich DPRs may reduce PM supply.

The supply of proteins and lipids to the PM in dendrites may in part be mediated by GOPs (Horton et al., 2005; Ye et al., 2007). GOPs are also essential for proper dendritic morphology (Horton et al., 2005; Ori-McKenney et al., 2012; Ye et al., 2007), and alteration in their number or location has been associated with dendritic defects in animal models for Parkinson's and several polyglutamine (polyQ) diseases (Chung et al., 2017; Lin et al., 2015). Based on these facts, we hypothesized that GOPs might be involved in dendritic defects caused by arginine-rich DPR toxicity. To test this, we expressed *PR36* in C4 da neurons along with the *medial*-Golgi marker, *ManII-eGFP*, and compared the number of GOPs to controls (Fig. 2C). We found that the number of GOPs marked by ManII-eGFP decreased significantly in *PR36*-expressing neurons compared to the controls (Fig. 2D). Similar results were obtained when we expressed the *trans*-Golgi marker *GalT-RFP* instead of *ManII-eGFP* (Supplementary Fig. S3). *GR36* expression also led to a significant reduction in the number of GOPs (Supplementary Figs. S4A and S4B), similar to the level caused by *PR36* expression. These data suggest that arginine-rich DPR toxicity leads to a reduction in the number of GOPs.

Nuclear PR toxicity induces down-regulation of *CrebA* mRNA expression

Previous studies have shown that GOPs can be regulated by secretory pathway-related genes (Chung et al., 2017; Iyer et al., 2013; Ye et al., 2007). CrebA is known to be a master regulator of the secretory pathway (Fox et al., 2010), and its expression is down-regulated by polyQ toxicity (Chung et al., 2017). Interestingly, a few studies have suggested that expression of aberrant proteins in the nucleus can lead to generalized toxicity, one sign of which is the sequestration of CBP (Fu et al., 2005; McCampbell et al., 2000; Nucifora et al., 2001; Steffan et al., 2000); *CrebA* is a downstream molecule of CBP (Chung et al., 2017). Because PR36 localizes predominantly in the nucleus of C4 da neurons (Figs. 3A and 3B), we hypothesized that nuclear toxicity induced by PR36 may alter the level of *CrebA* mRNA. To test this, we expressed *PR36* in *Drosophila* brains via the *elav-gal4* driver and measured the amount of *CrebA* mRNA in fly heads with respect to controls. RT-PCR showed that *PR36* expression led to a significant decrease in the level of *CrebA* mRNA compared to controls (Figs. 3C and 3D). However, unlike *PR36*, *GR36* expression did not induce changes in *CrebA* mRNA level (Supplementary Figs. S4C and S4D).

CrebA overexpression restores PM supply and the number of GOPs in C4 da neurons showing PR toxicity

If down-regulation of *CrebA* is involved in *PR36*-induced dendritic defects, its overexpression might restore some of those defects. We first confirmed that *CrebA* overexpression alone increased the number of GOPs (Figs. 4A and 4B) in C4 da neuronal dendrites, consistent with the results from a previous study (Chung et al., 2017). When *CrebA* was over-

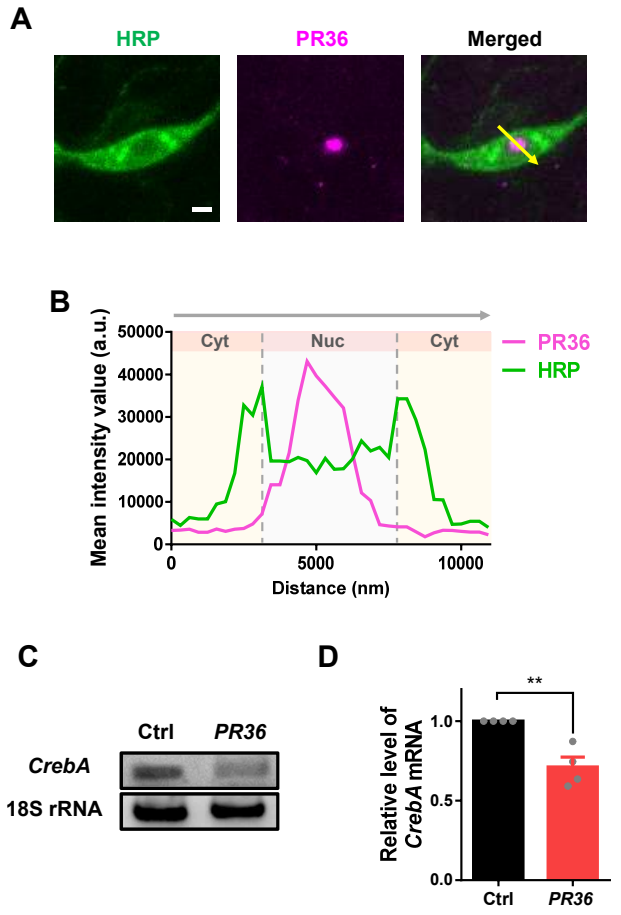

Fig. 3. Nuclear PR36 toxicity down-regulates *CrebA* mRNA expression. (A) Subcellular localization of PR36 (magenta) in C4 da neurons expressing *PR36* (Genotype: *UAS-PR36/+;ppk*^{1a}*-gal4/+*). HRP (green) indicate membrane marker. Scale bar = 5 μm. (B) The Intensitiy profiles of fluorescent signals representing PR36 (magenta) and HRP (green) across cell bodies along yellow arrow presented at Fig. 3A. The gray dashed lines indicate border of nuclei. (C) The amount of mRNA level of *CrebA* and 18S rRNA in the brain of Ctrl or expressing *PR36* (Genotype: **Ctrl**, *+/+;elav-gal4/+*; ***PR36***, *UAS-PR36/+;elav-gal4/+*). (D) Quantification of the mRNA level of *CrebA*. The values were normalized by those of 18S rRNA. $**P = 0.0036$ by two-tailed *t*-test; error bars ± SEM; n = 4 replicates.

expressed in *PR36*-expressing C4 da neurons, the number of GOPs was significantly increased compared to when *PR36* was expressed alone (Figs. 4A and 4B). The quantitative analysis suggests that the effect of *CrebA* and *PR36* on GOPs seems to be non-additive. Restoration of the GOP number suggests that the PM supply may also have been restored. To test this hypothesis, we examined the fluorescence intensity of CD4-tdGFP as a proxy for PM supply. *CrebA* overexpression alone increased the fluorescence intensity of CD4-tdGFP in C4 da neuronal dendrites (Figs. 4C and 4D), consistent with the previous study (Chung et al., 2017). When *CrebA* was overexpressed in *PR36*-expressing C4 da neurons, the fluorescence intensity of CD4-tdGFP was recovered to a normal level (Figs. 4C and 4D), implying that PM supply had been restored. However, the quantitative analysis indicates that the effect of *CrebA* and *PR36* on the PM supply seems to be additive, calling into question the relevance of CrebA to the PR36-induced PM supply defects. *CrebA* overexpression also did not change the number of dendritic branch points and the length of total dendrites in C4 da neurons expressing *PR36* (Supplementary Fig. S5). In addition, *CrebA* overexpression in adult fly retina could not mitigate PR36-induced degeneration (Supplementary Fig. S6). Notably, a similar pattern of restoration was observed in a polyQ disease fly model, where overexpression of *CrebA* restored GOP number and the fluorescence intensity of the PM marker, but not dendritic morphology in C4 da neurons (Chung et al., 2017). Taken together, these data suggest that multiple mechanisms underlie dendritic defects induced by PR toxicity and that *CrebA* overexpression alone cannot resolve all dendritic problems as was previously shown for polyQ toxicity (Chung et al., 2017).

DISCUSSION

In this study, we show that *C9orf72*-associated arginine-rich DPRs reduce the number of GOPs and dendritic branch points as well as PM supply in C4 da neurons. Mechanistically, *PR36* expression decreases *CrebA* mRNA level, the overexpression of which restores PM supply and the number of GOPs. To our knowledge, this is the first time that dendritic defects and loss of GOPs have been linked to arginine-rich DPR toxicity.

Golgi pathology has been observed in a number of neurodegenerative diseases and is considered to be one of the early features of neurodegeneration (Caracci et al., 2019; Gonatas et al., 2006). However, whether GOPs, which are unique to neuronal dendrites, are associated with neurodegenerative diseases has been understudied. Two recent studies showed GOP abnormalities in *Drosophila* models for Parkinson's and polyglutamine diseases (Chung et al., 2017; Lin et al., 2015), but whether they trigger neurodegeneration remains uncertain. In this study, we showed that although *CrebA* overexpression restored the number of GOPs and PM supply, it could not rescue PR-induced neurodegeneration of *Drosophila* retina (Supplementary Fig. S6). These data suggest that neurodegeneration may be caused by something other than defects in GOPs and PM supply. Previously, a link between PM supply (a function of Golgi) and neurodegenerative diseases such as Huntington's and Charcot–Marie–Tooth was suggested (Pfenninger, 2009). However, to our knowledge, no direct evidence indicating that defects in PM supply directly cause neurodegeneration has been reported. Therefore, further investigation of the role of GOPs and PM supply in neurodegeneration and dendritic pathology of other neurodegenerative diseases is warranted.

We show that *PR36* expression decreases the level of *CrebA* mRNA, but the mechanism by which this happens remains unknown. Previous studies showed that nucleus-accumulated polyQ (McCampbell et al., 2000; Nucifora et al., 2001; Steffan et al., 2000) and non-polyQ proteins (Fu et al., 2005) sequester CBP, which may reduce the transcription of its downstream factors such as *CrebA* (Chung et al., 2017).

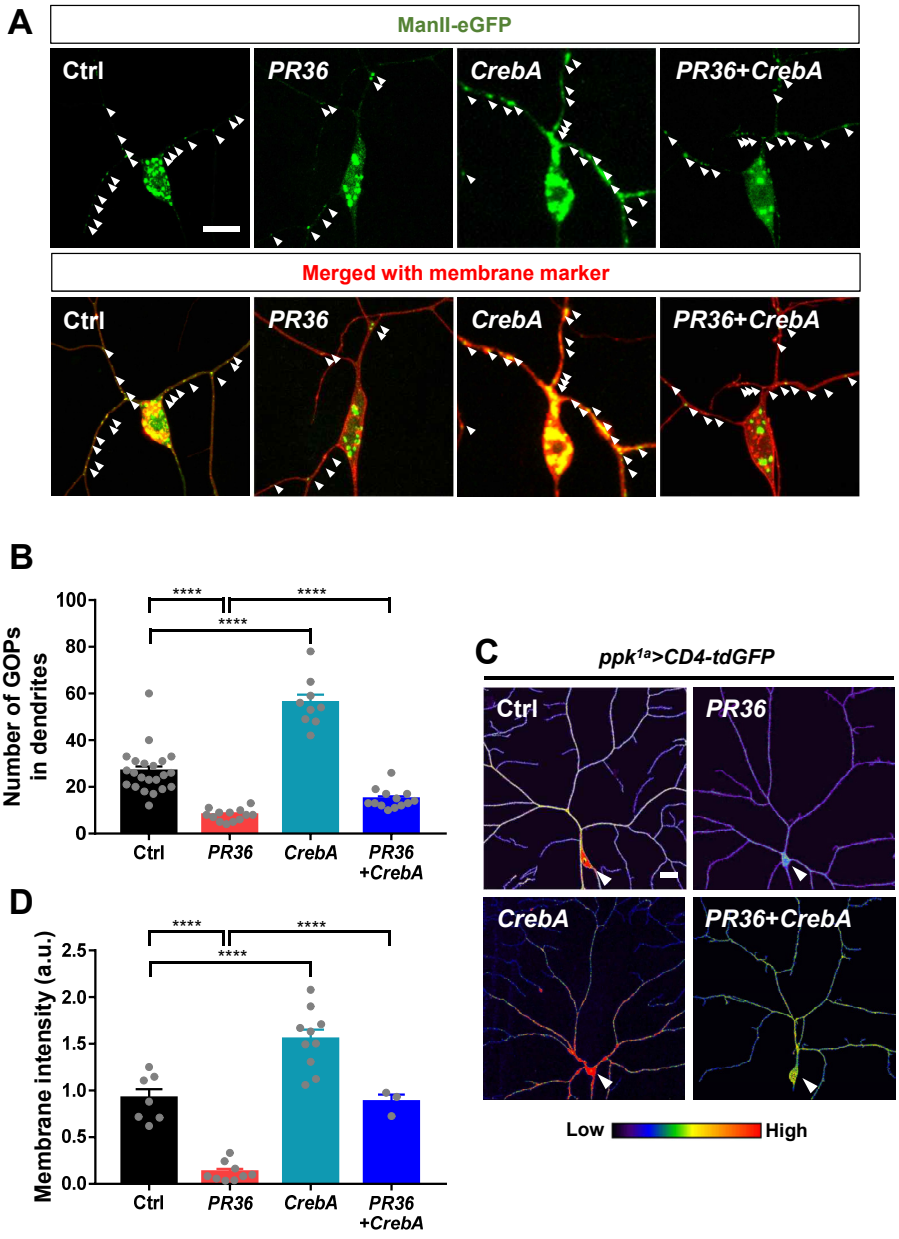

Fig. 4. Up-regulation of *CrebA* restores the number of GOPs and PM supply in C4 da neurons expressing *PR36*. (A) Representative images of GOPs (marked by *medial*-Golgi marker ManII-eGFP) in C4 da neurons of Ctrl or expressing *PR36*, *CrebA*, or *PR36* + *CrebA* (Genotype: **Ctrl**, *UAS-ManII-eGFP/+;ppk^{1a}>UAS-CD4-tdTOM/+*; ***PR36***, *UAS-PR36/UAS-ManII-eGFP;ppk^{1a}>UAS-CD4-tdTOM/+*; ***CrebA***, *UAS-CrebA/UAS-ManII-eGFP;ppk^{1a}>UAS-CD4-tdTOM/+*; ***PR36 + CrebA***, *UAS-PR36/UAS-CrebA,UAS-ManII-eGFP;ppk^{1a}>UAS-CD4-tdTOM/+*). White arrowheads indicate GOPs. Scale bar = 10 μm. (B) Quantification of the number of GOPs in C4 da neurons of Ctrl or expressing *PR36*, *CrebA*, or *PR36* + *CrebA* as described in Fig. 4A. ****$P < 0.0001$ by two-tailed *t*-test; error bars ± SEM; n = 13 neurons. (C) Representative CD4-tdGFP-labeled dendrite images (pseudo-colored) in C4 da neurons expressing the denoted transgenes (Genotype: **Ctrl**, *+/+;ppk^{1a}>UAS-CD4-tdGFP/+*; ***PR36***, *UAS-PR36/+;ppk^{1a}>UAS-CD4-tdGFP/+*; ***CrebA***, *UAS-CrebA/+;ppk^{1a}>UAS-CD4-tdGFP/+*; ***PR36 + CrebA***, *UAS-PR36/UAS-CrebA;ppk^{1a}>UAS-CD4-tdGFP/+*). White arrowheads indicate soma of neurons. Scale bar = 20 μm. (D) Quantification of the intensity value of CD4-tdGFP in C4 da neurons expressing the denoted transgenes described in Fig. 4C. ****$P <$ 0.0001 by two-tailed *t*-test; error bars ± SEM; n ≥ 3 neurons.

PR also localizes mostly in the nucleus (Figs. 3A and 3B), suggesting that PR may interfere with the function of CBP and subsequently reduce *CrebA* mRNA transcription. Another molecule through which *CrebA* might be down-regulated by PR toxicity is Ataxin-2 (Atx2). A knockdown of *Atx2* was recently shown to reduce the level of *CrebA* mRNA in *Drosoph-*

ila lateral neurons at dawn (Xu et al., 2019). Interestingly, Atx2 physically interacts with PR (Lee et al., 2016; Yin et al., 2017), suggesting that PR may interfere with Atx2 function through direct interaction and lead to a subsequent reduction in *CrebA* mRNA level.

Previous studies have shown that *PR* and *GR* disrupt a number of the same cellular processes including membraneless organelle dynamics (Lee et al., 2016), nucleocytoplasmic transport (Hayes et al., 2020), and RNA decay (Sun et al., 2020). This suggests that PR36 and GR36 might share a similar cellular mechanism that underlies dendritic defects in C4 da neurons. Indeed, we found that both *PR36* and *GR36* expression led to a significant reduction in the number of GOPs (Figs. 2A and 2B, Supplementary Figs. S4A and S4B). However, only *PR36* induced changes in *CrebA* mRNA level (Figs. 3C and 3D). These results suggest that although the cellular processes disrupted by PR and GR repeats may converge, the molecular mechanism underlying the disruptions likely diverge.

Defective vesicular trafficking in ALS/FTD has been observed in a number of disease models including those with mutations in *VAPB, CHMP2B, TMEM106B,* and *C9orf72* (Burk and Pasterkamp, 2019). For instance, a mutation of *Vap33* (a *Drosophila* ortholog of *VAPB*) in *Drosophila* has been shown to induce accumulation of phosphatidylinositol-4-phosphate in Golgi and lead to increased production of endosomes and impaired lysosomal degradation (Mao et al., 2019). In mouse cortical neurons, a mutation of *CHMP2B* has been shown to disrupt neuronal endolysosomal trafficking in such a manner that can be rescued by knockdown of *TMEM106B* (Clayton et al., 2018). Moreover, C9orf72 has been shown to interact with key components of the COPII pathway, such as Rab1 and Sec24, and may modulate the pathway (Burk and Pasterkamp, 2019; Farg et al., 2014; Goodier et al., 2020). Interestingly, synergistic toxicity between *C9orf72* haploinsufficiency and DPR toxicity has recently been suggested (Boivin et al., 2020; Shi et al., 2018; Zhu et al., 2020). Thus, we propose that haploinsufficiency and arginine-rich DPRs may synergistically target GOPs and lead to defective vesicular trafficking in dendrites.

Spinocerebellar ataxia 36 (SCA36) is caused by a hexanucleotide expansion repeat in the intron of *NOP56* gene (Kobayashi et al., 2011), the nucleotide sequence of which is TG3C2—remarkably similar to G4C2. A recent study showed that the expression of TG3C2 repeats in mice induced a loss of dendritic arbor in Purkinje cells (Todd et al., 2020), and the repeats were found to undergo RAN translation to produce PR and GP repeats in SCA36 patients (McEachin et al., 2020; Todd et al., 2020). Among the non-coding repeat expansion disorders, only SCA36 and C9-ALS/FTD manifest motor neuron degeneration (Ikeda et al., 2012; Kobayashi et al., 2011; Swinnen et al., 2020), suggesting that they may share a pathogenic mechanism. Although we have not tested GP repeats, *GP* expression is known to be mostly non-toxic in a number of model systems (Freibaum and Taylor, 2017). Thus, we propose that PR repeats may be the shared pathogenic driver underlying dendritic defects in these diseases. We envisage that further studies comparing the mechanistic similarity between SCA36 and C9-ALS/FTD using PR repeats will aid in developing new therapeutic targets for these diseases.

Note: Supplementary information is available on the Molecules and Cells website (www.molcells.org).

ACKNOWLEDGMENTS

This work was funded by Basic Science Research Program through the National Research Foundation of Korea, funded by the Ministry of Science and ICT (2018R1A2B6001607 and 2019R1A4A1024278) (to S.B.L.); the Development of Platform Technology for Innovative Medical Measurements Program from the Korea Research Institute of Standards and Science Grant (KRISS-2019-GP2019-0018) (to S.B.L.); and KBRI basic research program through Korea Brain Research Institute funded by Ministry of Science and ICT (20-BR-04-02) (to S.B.L.). The funders had no role in study design, data collection and analysis, decision to publish, or preparation of the manuscript.

AUTHOR CONTRIBUTIONS

J.H.P., C.G.C., and J.H.K. wrote the manuscript. J.H.P., C.G.C., and J.H.K. performed experiments. J.H.P., C.G.C., and J.H.K. analyzed the data. J.S., B.H.L., Y.S.L., and S.B.L. provided expertise and feedback. S.B.L. supervised the research.

CONFLICT OF INTEREST

The authors have no potential conflicts of interest to disclose.

ORCID

Jeong Hyang Park https://orcid.org/0000-0002-7392-8366
Chang Geon Chung https://orcid.org/0000-0001-8155-4926
Jinsoo Seo https://orcid.org/0000-0001-6432-6964
Byung-Hoon Lee https://orcid.org/0000-0002-7101-0471
Young-Sam Lee https://orcid.org/0000-0002-4702-0127
Jung Hyun Kweon https://orcid.org/0000-0002-0144-6157
Sung Bae Lee https://orcid.org/0000-0002-8980-6769

REFERENCES

Boivin, M., Pfister, V., Gaucherot, A., Ruffenach, F., Negroni, L., Sellier, C., and Charlet-Berguerand, N. (2020). Reduced autophagy upon C9ORF72 loss synergizes with dipeptide repeat protein toxicity in G4C2 repeat expansion disorders. EMBO J. *39*, e100574.

Burk, K. and Pasterkamp, R.J. (2019). Disrupted neuronal trafficking in amyotrophic lateral sclerosis. Acta Neuropathol. *137*, 859-877.

Caracci, M.O., Fuentealba, L.M., and Marzolo, M.P. (2019). Golgi complex dynamics and its implication in prevalent neurological disorders. Front. Cell Dev. Biol. *7*, 75.

Chung, C.G., Kwon, M.J., Jeon, K.H., Hyeon, D.Y., Han, M.H., Park, J.H., Cha, I.J., Cho, J.H., Kim, K., Rho, S., et al. (2017). Golgi outpost synthesis impaired by toxic polyglutamine proteins contributes to dendritic pathology in neurons. Cell Rep. *20*, 356-369.

Clayton, E.L., Milioto, C., Muralidharan, B., Norona, F.E., Edgar, J.R., Soriano, A., Jafar-Nejad, P., Rigo, F., Collinge, J., and Isaacs, A.M. (2018). Frontotemporal dementia causative CHMP2B impairs neuronal endolysosomal traffic-rescue by TMEM106B knockdown. Brain *141*, 3428-3442.

DeJesus-Hernandez, M., Mackenzie, I.R., Boeve, B.F., Boxer, A.L., Baker, M., Rutherford, N.J., Nicholson, A.M., Finch, N.A., Flynn, H., Adamson, J., et al.

(2011). Expanded GGGGCC hexanucleotide repeat in noncoding region of C9ORF72 causes chromosome 9p-linked FTD and ALS. Neuron *72*, 245-256.

Farg, M.A., Sundaramoorthy, V., Sultana, J.M., Yang, S., Atkinson, R.A., Levina, V., Halloran, M.A., Gleeson, P.A., Blair, I.P., Soo, K.Y., et al. (2014). C9ORF72, implicated in amytrophic lateral sclerosis and frontotemporal dementia, regulates endosomal trafficking. Hum. Mol. Genet. *23*, 3579-3595.

Ferrer, I. (1999). Neurons and their dendrites in frontotemporal dementia. Dement. Geriatr. Cogn. Disord. *10* Suppl 1, 55-60.

Fischer, L.R. and Glass, J.D. (2007). Axonal degeneration in motor neuron disease. Neurodegener. Dis. *4*, 431-442.

Fox, R.M., Hanlon, C.D., and Andrew, D.J. (2010). The CrebA/Creb3-like transcription factors are major and direct regulators of secretory capacity. J. Cell Biol. *191*, 479-492.

Freibaum, B.D. and Taylor, J.P. (2017). The Role of dipeptide repeats in C9ORF72-related ALS-FTD. Front. Mol. Neurosci. *10*, 35.

Fu, L., Gao, Y.S., and Sztul, E. (2005). Transcriptional repression and cell death induced by nuclear aggregates of non-polyglutamine protein. Neurobiol. Dis. *20*, 656-665.

Gonatas, N.K., Stieber, A., and Gonatas, J.O. (2006). Fragmentation of the Golgi apparatus in neurodegenerative diseases and cell death. J. Neurol. Sci. *246*, 21-30.

Goodier, J.L., Soares, A.O., Pereira, G.C., DeVine, L.R., Sanchez, L., Cole, R.N., and García-Pérez, J.L. (2020). C9orf72-associated SMCR8 protein binds in the ubiquitin pathway and with proteins linked with neurological disease. Acta Neuropathol. Commun. *8*, 110.

Hayes, L.R., Duan, L., Bowen, K., Kalab, P., and Rothstein, J.D. (2020). C9orf72 arginine-rich dipeptide repeat proteins disrupt karyopherin-mediated nuclear import. eLife *9*, e51685.

Herzog, J.J., Deshpande, M., Shapiro, L., Rodal, A.A., and Paradis, S. (2017). TDP-43 misexpression causes defects in dendritic growth. Sci. Rep. *7*, 15656.

Horton, A.C., Racz, B., Monson, E.E., Lin, A.L., Weinberg, R.J., and Ehlers, M.D. (2005). Polarized secretory trafficking directs cargo for asymmetric dendrite growth and morphogenesis. Neuron *48*, 757-771.

Ikeda, Y., Ohta, Y., Kobayashi, H., Okamoto, M., Takamatsu, K., Ota, T., Manabe, Y., Okamoto, K., Koizumi, A., and Abe, K. (2012). Clinical features of SCA36: a novel spinocerebellar ataxia with motor neuron involvement (Asidan). Neurology *79*, 333-341.

Iyer, S.C., Ramachandran Iyer, E.P., Meduri, R., Rubaharan, M., Kuntimaddi, A., Karamsetty, M., and Cox, D.N. (2013). Cut, via CrebA, transcriptionally regulates the COPII secretory pathway to direct dendrite development in Drosophila. J. Cell Sci. *126*, 4732-4745.

Jan, Y.N. and Jan, L.Y. (2010). Branching out: mechanisms of dendritic arborization. Nat. Rev. Neurosci. *11*, 316-328.

Karpati, G., Carpenter, S., and Durham, H. (1988). A hypothesis for the pathogenesis of amyotrophic lateral sclerosis. Rev. Neurol. (Paris) *144*, 672-675.

Kobayashi, H., Abe, K., Matsuura, T., Ikeda, Y., Hitomi, T., Akechi, Y., Habu, T., Liu, W., Okuda, H., and Koizumi, A. (2011). Expansion of intronic GGCCTG hexanucleotide repeat in NOP56 causes SCA36, a type of spinocerebellar ataxia accompanied by motor neuron involvement. Am. J. Hum. Genet. *89*, 121-130.

Kulkarni, V.A. and Firestein, B.L. (2012). The dendritic tree and brain disorders. Mol. Cell. Neurosci. *50*, 10-20.

Kweon, J.H., Kim, S., and Lee, S.B. (2017). The cellular basis of dendrite pathology in neurodegenerative diseases. BMB Rep. *50*, 5-11.

Kwon, I., Xiang, S., Kato, M., Wu, L., Theodoropoulos, P., Wang, T., Kim, J., Yun, J., Xie, Y., and McKnight, S.L. (2014). Poly-dipeptides encoded by the C9orf72 repeats bind nucleoli, impede RNA biogenesis, and kill cells. Science *345*, 1139-1145.

Kwon, M.J., Han, M.H., Bagley, J.A., Hyeon, D.Y., Ko, B.S., Lee, Y.M., Cha, I.J., Kim, S.Y., Kim, D.Y., Kim, H.M., et al. (2018). Coiled-coil structure-dependent interactions between polyQ proteins and Foxo lead to dendrite pathology and behavioral defects. Proc. Natl. Acad. Sci. U. S. A. *115*, E10748-E10757.

Lee, K.H., Zhang, P., Kim, H.J., Mitrea, D.M., Sarkar, M., Freibaum, B.D., Cika, J., Coughlin, M., Messing, J., Molliex, A., et al. (2016). C9orf72 dipeptide repeats impair the assembly, dynamics, and function of membrane-less organelles. Cell *167*, 774-788.e17.

Lee, S.B., Bagley, J.A., Lee, H.Y., Jan, L.Y., and Jan, Y.N. (2011). Pathogenic polyglutamine proteins cause dendrite defects associated with specific actin cytoskeletal alterations in Drosophila. Proc. Natl. Acad. Sci. U. S. A. *108*, 16795-16800.

Lee, Y.B., Chen, H.J., Peres, J.N., Gomez-Deza, J., Attig, J., Stalekar, M., Troakes, C., Nishimura, A.L., Scotter, E.L., Vance, C., et al. (2013). Hexanucleotide repeats in ALS/FTD form length-dependent RNA foci, sequester RNA binding proteins, and are neurotoxic. Cell Rep. *5*, 1178-1186.

Lin, C.H., Li, H., Lee, Y.N., Cheng, Y.J., Wu, R.M., and Chien, C.T. (2015). Lrrk regulates the dynamic profile of dendritic Golgi outposts through the golgin Lava lamp. J. Cell Biol. *210*, 471-483.

Ling, S.C., Polymenidou, M., and Cleveland, D.W. (2013). Converging mechanisms in ALS and FTD: disrupted RNA and protein homeostasis. Neuron *79*, 416-438.

Mao, D., Lin, G., Tepe, B., Zuo, Z., Tan, K.L., Senturk, M., Zhang, S., Arenkiel, B.R., Sardiello, M., and Bellen, H.J. (2019). VAMP associated proteins are required for autophagic and lysosomal degradation by promoting a PtdIns4P-mediated endosomal pathway. Autophagy *15*, 1214-1233.

McCampbell, A., Taylor, J.P., Taye, A.A., Robitschek, J., Li, M., Walcott, J., Merry, D., Chai, Y., Paulson, H., Sobue, G., et al. (2000). CREB-binding protein sequestration by expanded polyglutamine. Hum. Mol. Genet. *9*, 2197-2202.

McEachin, Z.T., Gendron, T.F., Raj, N., Garcia-Murias, M., Banerjee, A., Purcell, R.H., Ward, P.J., Todd, T.W., Merritt-Garza, M.E., Jansen-West, K., et al. (2020). Chimeric peptide species contribute to divergent dipeptide repeat pathology in c9ALS/FTD and SCA36. Neuron *107*, 292-305.e6.

Murthy, M., Ranjan, R., Denef, N., Higashi, M.E., Schupbach, T., and Schwarz, T.L. (2005). Sec6 mutations and the Drosophila exocyst complex. J. Cell Sci. *118*, 1139-1150.

Nakano, I. and Hirano, A. (1987). Atrophic cell processes of large motor neurons in the anterior horn in amyotrophic lateral sclerosis: observation with silver impregnation method. J. Neuropathol. Exp. Neurol. *46*, 40-49.

Nucifora, F.C., Jr., Sasaki, M., Peters, M.F., Huang, H., Cooper, J.K., Yamada, M., Takahashi, H., Tsuji, S., Troncoso, J., Dawson, V.L., et al. (2001). Interference by huntingtin and atrophin-1 with cbp-mediated transcription leading to cellular toxicity. Science *291*, 2423-2428.

Ori-McKenney, K.M., Jan, L.Y., and Jan, Y.N. (2012). Golgi outposts shape dendrite morphology by functioning as sites of acentrosomal microtubule nucleation in neurons. Neuron *76*, 921-930.

Pfenninger, K.H. (2009). Plasma membrane expansion: a neuron's Herculean task. Nat. Rev. Neurosci. *10*, 251-261.

Renton, A.E., Majounie, E., Waite, A., Simon-Sanchez, J., Rollinson, S., Gibbs, J.R., Schymick, J.C., Laaksovirta, H., van Swieten, J.C., Myllykangas, L., et al. (2011). A hexanucleotide repeat expansion in C9ORF72 is the cause of chromosome 9p21-linked ALS-FTD. Neuron *72*, 257-268.

Rudich, P., Snoznik, C., Watkins, S.C., Monaghan, J., Pandey, U.B., and Lamitina, S.T. (2017). Nuclear localized C9orf72-associated arginine-containing dipeptides exhibit age-dependent toxicity in C. elegans. Hum. Mol. Genet. *26*, 4916-4928.

Saberi, S., Stauffer, J.E., Schulte, D.J., and Ravits, J. (2015). Neuropathology of amyotrophic lateral sclerosis and its variants. Neurol. Clin. *33*, 855-876.

Shi, Y., Lin, S., Staats, K.A., Li, Y., Chang, W.H., Hung, S.T., Hendricks, E., Linares, G.R., Wang, Y., Son, E.Y., et al. (2018). Haploinsufficiency leads to neurodegeneration in C9ORF72 ALS/FTD human induced motor neurons. Nat. Med. *24*, 313-325.

Steffan, J.S., Kazantsev, A., Spasic-Boskovic, O., Greenwald, M., Zhu, Y.Z., Gohler, H., Wanker, E.E., Bates, G.P., Housman, D.E., and Thompson, L.M. (2000). The Huntington's disease protein interacts with p53 and CREB-binding protein and represses transcription. Proc. Natl. Acad. Sci. U. S. A. *97*, 6763-6768.

Sun, Y., Eshov, A., Zhou, J., Isiktas, A.U., and Guo, J.U. (2020). C9orf72 arginine-rich dipeptide repeats inhibit UPF1-mediated RNA decay via translational repression. Nat. Commun. *11*, 3354.

Swinnen, B., Robberecht, W., and Van Den Bosch, L. (2020). RNA toxicity in non-coding repeat expansion disorders. EMBO J. *39*, e101112.

Takeda, T., Uchihara, T., Nakayama, Y., Nakamura, A., Sasaki, S., Kakei, S., Uchiyama, S., Duyckaerts, C., and Yoshida, M. (2014). Dendritic retraction, but not atrophy, is consistent in amyotrophic lateral sclerosis-comparison between Onuf's neurons and other sacral motor neurons. Acta Neuropathol. Commun. *2*, 11.

Taylor, J.P., Brown, R.H., Jr., and Cleveland, D.W. (2016). Decoding ALS: from genes to mechanism. Nature *539*, 197-206.

Tibshirani, M., Zhao, B., Gentil, B.J., Minotti, S., Marques, C., Keith, J., Rogaeva, E., Zinman, L., Rouaux, C., Robertson, J., et al. (2017). Dysregulation of chromatin remodelling complexes in amyotrophic lateral sclerosis. Hum. Mol. Genet. *26*, 4142-4152.

Todd, T.W., McEachin, Z.T., Chew, J., Burch, A.R., Jansen-West, K., Tong, J., Yue, M., Song, Y., Castanedes-Casey, M., Kurti, A., et al. (2020). Hexanucleotide repeat expansions in c9FTD/ALS and SCA36 confer selective patterns of neurodegeneration in vivo. Cell Rep. *31*, 107616.

Wen, X., Tan, W., Westergard, T., Krishnamurthy, K., Markandaiah, S.S., Shi, Y., Lin, S., Shneider, N.A., Monaghan, J., Pandey, U.B., et al. (2014). Antisense proline-arginine RAN dipeptides linked to C9ORF72-ALS/FTD form toxic nuclear aggregates that initiate in vitro and in vivo neuronal death. Neuron *84*, 1213-1225.

Xu, F., Kula-Eversole, E., Iwanaszko, M., Lim, C., and Allada, R. (2019). Ataxin2 functions via CrebA to mediate Huntingtin toxicity in circadian clock neurons. PLoS Genet. *15*, e1008356.

Xu, Z., Poidevin, M., Li, X., Li, Y., Shu, L., Nelson, D.L., Li, H., Hales, C.M., Gearing, M., Wingo, T.S., et al. (2013). Expanded GGGGCC repeat RNA associated with amyotrophic lateral sclerosis and frontotemporal dementia causes neurodegeneration. Proc. Natl. Acad. Sci. U. S. A. *110*, 7778-7783.

Ye, B., Zhang, Y., Song, W., Younger, S.H., Jan, L.Y., and Jan, Y.N. (2007). Growing dendrites and axons differ in their reliance on the secretory pathway. Cell *130*, 717-729.

Yin, S., Lopez-Gonzalez, R., Kunz, R.C., Gangopadhyay, J., Borufka, C., Gygi, S.P., Gao, F.B., and Reed, R. (2017). Evidence that C9ORF72 dipeptide repeat proteins associate with U2 snRNP to cause mis-splicing in ALS/FTD patients. Cell Rep. *19*, 2244-2256.

Zhu, Q., Jiang, J., Gendron, T.F., McAlonis-Downes, M., Jiang, L., Taylor, A., Diaz Garcia, S., Ghosh Dastidar, S., Rodriguez, M.J., King, P., et al. (2020). Reduced C9ORF72 function exacerbates gain of toxicity from ALS/FTD-causing repeat expansion in C9orf72. Nat. Neurosci. *23*, 615-624